Polarizability measurements of a molecule via a near-field matter-wave interferometer

Martin Berninger, André Stefanov, Sarayut Deachapunya, and Markus Arndt*
Fakultät für Physik der Universität Wien, Boltzmanngasse 5, A–1090 Wien, Austria
(Received 11 December 2006; published 9 July 2007)

We present a method for measuring the scalar polarizability of molecules by means of near-field matter-wave interferometry. This technique is applicable to a wide range of complex neutral molecules. A key feature of our experiment is the combination of good transmission and high spatial resolution, gained by imprinting a submicrometer spatial modulation onto a wide molecular beam. Our method significantly improves the measurement sensitivity of the polarizability-dependent shifts. We have successfully performed measurements on fullerenes and report the polarizability to be $\alpha=88.9\pm0.9\pm5.1$ Å^3 for C_{60} and $\alpha=108.5\pm2.0\pm6.2$ Å^3 for C_{70}.

DOI: 10.1103/PhysRevA.76.013607 PACS number(s): 03.75.Dg, 03.65.−w, 33.15.Kr

Knowing the scalar polarizability of a molecule is of importance in various areas of physics. The polarizability provides one of several parameters in the description of molecular structures and conformations [1]. Even for the structurally simple molecules C_{60} and C_{70}, various theoretical models are still competing with each other [2].

The molecular response to external electric fields is also a handle for slowing [3–5], cooling, or trapping [6] neutral particles in switched electric fields or off-resonant laser beams.

The polarizability turns out to be crucial also for matter-wave interferometry. It enters, for instance, in the physics of diffraction, through phase-shifting the van der Waals interactions between the molecules and the diffracting grating walls [7,8]. But it is also important for decoherence considerations. Polarizability-dependent small-angle scattering of residual gas molecules in the vacuum chamber may destroy the molecular coherence [9].

Finally, precise α measurements are also stimulated by the insight that future molecule interferometers will also exploit optical gratings [10–12], which induce a phase shift determined by the polarizability.

Various experimental approaches are conceivable to determine α with high precision [2]. In solids or liquids, the polarizability can be obtained through a measurement of the dielectric constant and the index of refraction [1]. But in particular for the comparison with theoretical models it is desirable to get information about the isolated particles [13].

Polarizabilities of dilute molecular beams are usually characterized in Stark-deflection experiments, in which the neutral molecules traverse a homogeneous electrostatic force field. The polarizability can then be determined by measuring the lateral shift of the molecular beam due to this field. In most experiments the resulting deflections are much smaller than the width of the molecular beam profile [2] but still such experiments can typically reach an accuracy of about 10% [14]. One may also consider the use of electric field gradients to induce a longitudinal velocity shift and corresponding time-of-flight delay in a molecular fountain arrangement [15].

For atoms, very precise polarizability values were also obtained using far-field matter-wave interferometry: the atomic wave function can be coherently split and guided through two spatially separated electric fields. The different phases imprinted on the atom through the interaction between α and electric field E along the two different paths shows up as a fringe shift that can be well resolved. This allowed a very accurate determination of ground-state polarizabilities for sodium [16] and lithium [17].

Efficient new methods are, however, desirable for metrology on large molecules, in particular since their α/m values may be significantly smaller than those of alkali-metal atoms. The use of far-field interferometry would, however, require beam sources of very high spatial coherence. In the absence of efficient cooling and phase-space compression methods, this can only be achieved by strictly collimating the molecular beam. Although we have successfully demonstrated far-field diffraction in our earlier work for large carbon molecules [18], the limited flux of almost all other large particles would prohibit such a strict spatial selection. While classical Stark deflection usually provides a high flux with a low spatial resolution, far-field interferometers trade their high resolution for a strongly restricted molecular transmission.

Here we report on a solution to this problem, which is based on a near-field Talbot-Lau interferometer (TLI). It combines high spatial resolution with high molecular throughput and it can even be generalized to objects of arbitrary mass—in the limit of classical Moiré deflectometry.

A Talbot-Lau interferometer uses near-field wave effects, generally for the lensless imaging of periodic nanostructures [19]. It has already been described earlier in the context of atom [20,21] and molecule [8,22] interferometry. In our present apparatus we employ a TLI composed of three gold gratings with a grating period of $g=991$ nm and slit openings of about 450 nm width.

The first grating prepares the required spatial coherence to obtain matter-wave diffraction at the second grating, which then results in a regular molecular density pattern, immediately in front of the mask grating. The interference fringes, whose periodicity equals the grating constant, can be revealed by scanning the third grating laterally. The resulting modulation of the molecular flux behind this setup allows one to visualize the molecular nanofringe system. The molecular beam width in a TL interferometer may be wider than 1 mm, allowing a high throughput of molecules while the

*markus.arndt@univie.ac.at

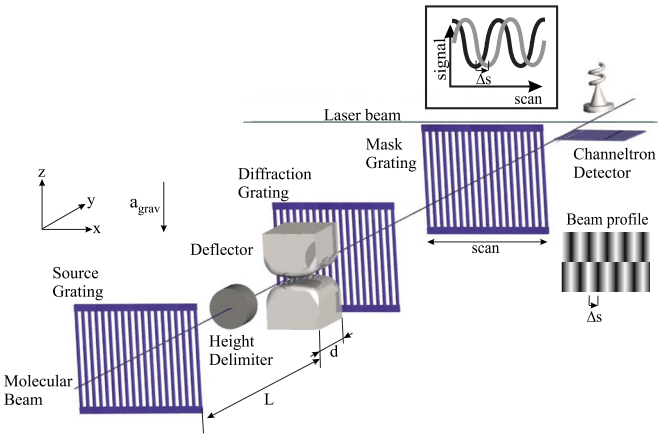

FIG. 1. (Color online) Experimental setup. The three gratings are used for coherence preparation, diffraction, and detection. Path-dependent matter-wave phase shifts in the external field lead to a deflection of the beam profile at the position of the mask grating. The lateral shift Δs of the interference fringes at the detector is directly proportional to the scalar molecular polarizability α.

resolution of the fringe system can be of the order of 15 nm, i.e., about 100 000 times better.

We now insert an electrostatic deflector into the TLI (see Fig. 1), which creates a homogeneous force field $\mathbf{F}=\alpha(\mathbf{E}\nabla)\mathbf{E}$ changing the momentum of the molecules in proportion to the applied electric field $\mathbf{E}$, its gradient $\nabla\mathbf{E}$, and the polarizability α. In the proper quantum picture, the electric field adds a path-dependent phase shift to the molecular matter wave. In both descriptions, classical and quantum, we obtain a fringe shift

$$\Delta s_x(\alpha,v) = \alpha\frac{(\mathbf{E}\nabla)E_x}{m}\frac{d}{v^2}\left(\frac{d}{2}+L\right), \tag{1}$$

where m corresponds to the molecular mass, v the velocity along the direction of the beam, and L the distance between the source grating and the deflector. The front edge of the deflector (length d) is positioned at $L=26.6\pm0.1$ cm behind the first grating. The deflector provides a constant force with deviations of 0.5% along the x axis over the entire molecular beam diameter.

Two interference recordings at two different deflection voltages would be sufficient to determine the molecular polarizability, if all parameters were known with arbitrary precision. Figure 2 shows a fringe system of C_{60} with a deflection voltage of 0 and 6 kV. The field-dependent shifts can be nicely resolved and measured with high accuracy. In order to obtain additional statistical information and to assess the accuracy of the various contributing parameters, we repeat the measurements for different velocity distributions and for different deflection voltages.

We employ a gravitational velocity selection [8,23] and chose the velocity by moving the source to its appropriate vertical position. An interference pattern is then recorded by displacing the third grating in steps of 20 nm over about three fringe periods and by repeating this scan for all voltages within 3–15 kV in steps of 1 kV.

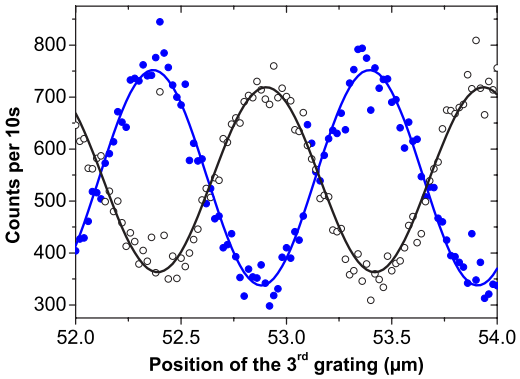

FIG. 2. (Color online) Deflection of a C_{60} beam with $\bar{v}=117$ m/s and $\sigma_v=8\%$. A phase shift of $\Delta\phi=\pi$ is obtained at a voltage of 6 kV (full circles). The open circles represent the reference at $U=0$ kV.

To monitor and numerically compensate for drifts, an additional reference point (with $U=0$ kV) is always included before and after each high-voltage deflection scan. From the interference curves thus obtained we extract the voltage dependence of the experimental fringe shift (Fig. 3).

The observed fringe shift is influenced by the details of the molecular velocity distribution in three ways. First, slow molecules will acquire a larger deflection in the external field gradient than fast ones [Eq. (1)]. Second, different velocity classes are associated with different visibilities. This is an important and desired feature of the Talbot-Lau arrangement, as it allows one to prove the quantum wave nature of material objects [8]. Third, the van der Waals interaction with the grating walls adds a dispersive phase shift [7,8].

The expected signal as a function of the scanning grating position x is proportional to

$$1+\bar{V}_{th}(\alpha)\cos\left(\frac{2\pi}{g}[x-\Delta s_{th}(\alpha)]\right) \equiv \int dv\, f_{\bar{v},\sigma_v}(v)\left[1+V(v)\cos\left(\frac{2\pi}{g}[x-\Delta s_x(\alpha,v)]\right)\right], \tag{2}$$

where the velocity distribution function $f_{\bar{v},\sigma_v}(v)$ is experi-

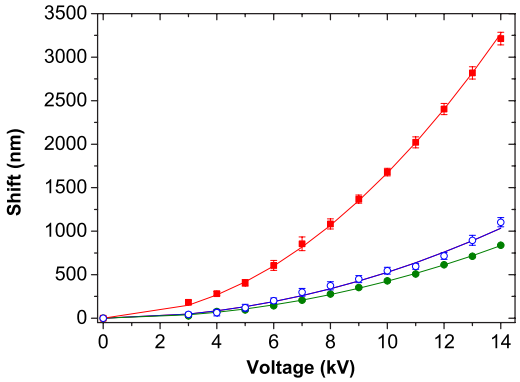

FIG. 3. (Color online) Stark deflection of the C_{70} fringes. It follows precisely the quadratic voltage dependence $\Delta s\propto U^2/v^2$ of Eq. (1): full circles, $\bar{v}=199$ m/s, $\sigma_v=16\%$; open circles, $\bar{v}=173$ m/s, $\sigma_v=13\%$; full squares, $\bar{v}=109$ m/s, $\sigma_v=7\%$.

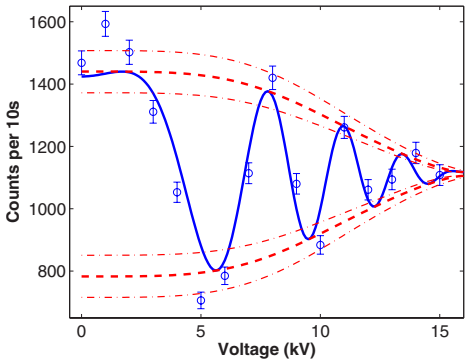

FIG. 4. (Color online) Signal as a function of the deflection voltage for a fixed position of the mask grating. The open circles are data points for C_{70} at a velocity of $\bar{v}=103.2$ m/s, $\sigma_v=7\%$. The solid line is the theoretical expectation for $\alpha=108.5$ Å^3. The dashed line is the envelope curve of the visibility function. The dash-dotted lines illustrate upper and lower bounds resulting from small variations of the velocity distribution, $\Delta\bar{v}=\pm1\%$, $\Delta\sigma_v=\pm1\%$, and typical uncertainties of the visibility, $\Delta V(v)=\pm3\%$.

mentally determined for several source settings, i.e., different mean velocities $\bar{v}$. The fringe visibility function $V(v)$ cannot be measured directly because of the finite width of the velocity distribution σ_v. It is extracted from the measured visibilities $V(\bar{v},\sigma_v)$ using

$$V(\bar{v},\sigma_v)=\int dv\, f_{\bar{v},\sigma_v}(v)V(v). \tag{3}$$

The polarizability α is then obtained by fitting the experimentally observed shift Δs_{expt} with the theoretical shift $\Delta s_{th}(\alpha)$.

We limit the maximum deflection voltage in the experiment to 15 kV since the fringes of slow (109 m/s) fullerenes are then already shifted by three entire periods (Fig. 3) and dephasing effects become important. Molecules of different velocities experience a different Stark deflection, and the summation over the corresponding molecule interference patterns in the detector will reduce the total fringe visibility for sufficiently large velocity spreads σ_v and with increasing voltage (see Fig. 4). In our experiments $\sigma_v(e^{-1/2})$ ranges between 7% and 16% for molecules between 100 and 200 m/s, respectively.

When all grating positions are fixed, the scanning deflection voltage can be used to sweep the molecular density pattern across the third grating (Fig. 4). The data points are well described using the implicit functions of the voltage for the expected visibility $\bar{V}_{th}(\alpha)$ and shift $\Delta s_{th}(\alpha)$. It is interesting to note that not only the shift but also the voltage-dependent dephasing, which leads to a rather sharp decrease in the interference contrast, may actually be used as tools for metrology. The fringe shifts are, however, less sensitive to additional random perturbations—such as vibrations, thermal radiation, or collisions—than the visibility, and the values given below are therefore based on the displacement measurements.

We find a polarizability of $88.9\pm0.9\pm5.1$ Å^3 for C_{60} and $108.5\pm2.0\pm6.2$ Å^3 for C_{70}, including the statistical (first) and systematic (second) error. The relative polarizability is then $\alpha(C_{70})/\alpha(C_{60})=1.22\pm0.03$. Most of the systematic uncertainties, such as, for instance, field inhomogeneities, cancel out in the determination of the relative values.

The statistical uncertainty of 2%, given above, refers to the standard deviation in the determination of α for different velocities. If all data were purely shot-noise limited, we would expect an uncertainty as small as 0.1%.

The uncertainty in the measurement of the velocity amounts to 1%; the voltages are known to 0.5%. The lateral resolution of our interferometer is currently good to within ~15 nm. This amounts to less than 0.5% of the maximum fringe shift, which corresponds to a lateral force sensitivity of better than 10^{-26} N.

The properties of the electric field are characterized using a finite-element code [24] which finds a value of $(\mathbf{E}\nabla)E_x=(1.45\pm0.08)\times10^{14}$ V^2/m^3 for a voltage of 10 kV. The same code is used to determine the effective electrode length $d_{eff}=4.73\pm0.1$ cm, which replaces the real electrode length because of edge effects. The remaining uncertainties comprise the accuracy in the measurement of the electrode's contour and separation. All independent systematic uncertainties add up to a total of 5.7%.

Our values for the polarizability are slightly larger than those of other static measurements in the gas phase, $\alpha(C_{60})=76.5\pm8.0$ Å^3 [14] and $\alpha(C_{70})=102\pm14$ Å^3 [2]. The ac-polarizability of isolated C_{60} interacting with an off-resonance neodymium-doped yttrium aluminium garnet, laser beam was determined to be $\alpha=79\pm4$ Å^3 [25]. Thin-film studies for C_{60} range from 84 to 93 Å^3, agreeing nicely with our measurements (for a review, see [1]). There is a broad range of theoretical values varying between 36 and 154 Å^3 [1,2], whereas our results are closest to calculations obtained by the bond polarizability model, $\alpha(C_{60})=89.2$ Å^3 and $\alpha(C_{70})=109.2$ Å^3 [26].

It is interesting to note that our apparatus may also be regarded as a fast switch for molecular beams. The fine structure imprinted on the beam by its transmission through the first two gratings allows us to lower and raise the molecular transmission with kilohertz-frequencies. In dedicated experiments it should be possible to reach a modulation amplitude of close to 100%.

In conclusion, we have demonstrated that a near-field matter-wave interferometer is a promising tool for sensitively measuring the scalar polarizability. The advantage of our approach is the independence of the shifted fringe pattern of the uncollimated molecular beam. This feature is the main difference from the polarizability measurements in the gas phase carried out so far, and would allow performance of precise experiments with complex molecules, where the count rates are generally low due to inefficient detection schemes. With respect to far-field interference methods the near-field scheme can be extrapolated to a large extent toward significantly more complex particles.

As mentioned before, the velocity spread is a critical parameter, since it enters quadratically in Eq. (1). However, in particular in pulsed molecular beam experiments, based on

laser desorption and on pulsed photoionization, the velocity selection can reach values as small as $\Delta v/v \sim 0.1\%$ at acceptable signal intensities [27], even if the entire beam still has a finite temperature. In this way it is already possible to generate neutral beams of fullerenes and complex biomolecules [14,28] up to polypeptides composed of 15 amino acids [27].

In biomolecules, the conformational variation of polarizabilities and electric dipole moments will be of interest. If the molecules exhibit a finite electric or magnetic dipole moment, the random orientation of cold molecules will lead to a decrease of the visibility instead of a simple fringe shift [29]. As mentioned above, the amount of dephasing will then allow the extraction of a numerical value for the moments. For hot molecular beams that possess a permanent electric dipole moment, the system behaves as an object with an induced polarizability [30], which should also be measurable in our setup.

The extension of our present setup to pulsed sources and detectors is particularly interesting, for instance, for investigating the temperature dependence of the molecular polarizability. But also magnetic moments or lifetimes of excited triplet states should be accessible in dedicated future experiments based on our present setup.

Our work is supported by the Austrian FWF through SFBF1505 and STARTY177-2, and the European Commission under Contract No. HPRN-CT-2002-00309. S.D. is supported by the Royal Thai Government. We thank H. Ulbricht for fruitful discussions.

[1] K. Bonin and V. Kresin, *Electric-Dipole Polarizabilities of Atoms, Molecules and Clusters* (World Scientific, Singapore, 1997).
[2] I. Compagnon, R. Antoine, M. Broyer, P. Dugourd, J. Lermé and D. Rayane, Phys. Rev. A **64**, 025201 (2001).
[3] J. A. Maddi, T. P. Dinneen, and H. Gould, Phys. Rev. A **60**, 3882 (1999).
[4] H. L. Bethlem, G. Berden, and G. Meijer, Phys. Rev. Lett. **83**, 1558 (1999).
[5] R. Fulton, A. I. Bishop, and P. F. Barker, Phys. Rev. Lett. **93**, 243004 (2004).
[6] T. Takekoshi, J. R. Yeh, and R. J. Knize, Opt. Commun. **114**, 421 (1995).
[7] R. E. Grisenti, W. Schöllkopf, J. P. Toennies, G. C. Hegerfeldt, and T. Köhler, Phys. Rev. Lett. **83**, 1755 (1999).
[8] B. Brezger, L. Hackermüller, S. Uttenthaler, J. Petschinka, M. Arnat, and A. Zeilinger, Phys. Rev. Lett. **88**, 100404 (2002).
[9] K. Hornberger, S. Uttenthaler, B. Brezger, L. Hackermüller, M. Arndt, and A. Zeilinger, Phys. Rev. Lett. **90**, 160401 (2003).
[10] P. L. Gould, G. A. Ruff, and D. E. Pritchard, Phys. Rev. Lett. **56**, 827 (1986).
[11] O. Nairz, B. Brezger, M. Arndt, and A. Zeilinger, Phys. Rev. Lett. **87**, 160401 (2001).
[12] B. Brezger, M. Arndt, and A. Zeilinger, J. Opt. B: Quantum Semiclassical Opt. **5**, S82 (2003).
[13] J. P. Simons, R. A. Jockusch, P. ÇarÇabal, I. Hünig, R. T. Kroemer, N. A. Macleod, and L. C. Snoek, Int. Rev. Phys. Chem. **24**, 489 (2005).
[14] R. Antoine, Ph. Dugourd, D. Rayane, E. Benichou, M. Broyer, F. Chandezon, and C. Guet, J. Chem. Phys. **110**, 9771 (1999).
[15] J. M. Amini and H. Gould, Phys. Rev. Lett. **91**, 153001 (2003).
[16] C. Ekstrom, J. Schiedmayer, M. S. Chapman, T. D. Hammond, and D. E. Pritchard, Phys. Rev. A **51**, 3883 (1995).
[17] A. Miffre, M. Jacquey, M. Büchner, G. Trénec, and J. Vigué, Phys. Rev. A **73**, 011603 (2006).
[18] M. Arndt, O. Nairz, J. Voss-Andreae, C. Keller, G. van der Zouw, and A. Zeilinger, Nature (London) **401**, 680 (1999).
[19] K. Patorski, Prog. Opt. **27**, 1 (1989).
[20] J. Clauser and M. Reinsch, Appl. Phys. B: Photophys. Laser Chem. **54**, 380 (1992).
[21] J. Clauser and S. Li, Phys. Rev. A **49**, R2213 (1994).
[22] L. Hackermüller, S. Uttenthaler, K. Hornberger, E. Reiger, B. Brezger, A. Zeilinger, and M. Arndt, Phys. Rev. Lett. **91**, 090408 (2003).
[23] M. Arndt, O. Nairz, J. Petschinka, and A. Zeilinger, C. R. Acad. Sci., Ser IV: Phys., Astrophys. **2**, 547 (2001).
[24] Computer code FEMLAB (Comsol, Stockholm, 2004).
[25] A. A. Ballard, K. Bonin, and J. Louderback, J. Chem. Phys. **113**, 5732 (2000).
[26] S. Guha, J. Menendez, J. B. Page, and G. B. Adams, Phys. Rev. B **53**, 13106 (1996).
[27] M. Marksteiner, G. Kiesewetter, L. Hackermüller, H. Ulbricht, and M. Arndt, Acta Phys. Hung. B **26**, 87 (2006).
[28] G. Meijer, M. S. de Vries, H. E. Hunziker, and H. R. Wendt, Appl. Phys. B: Photophys. Laser Chem. **51**, 395 (1990).
[29] R. Antoine, I. Compagnon, D. Rayane, M. Broyer, Ph. Dugourd, G. Breaux, F. C. Hagemeister, D. Pippen, R. R. Hudgins, and M. F. Jarrold, Eur. Phys. J. D **20**, 583 (2002).
[30] R. Moro, R. Rabinovitch, C. Xia, and V. V. Kresin, Phys. Rev. Lett. **97**, 123401 (2006).